Articles

A Unique Zinc-Binding Site Revealed by a High-Resolution X-ray Structure of Homotrimeric Apo2L/TRAIL

Sarah G. Hymowitz,‡ Mark P. O'Connell,‡ Mark H. Ultsch,‡ Amy Hurst,§ Klara Totpal,|| Avi Ashkenazi,⊥ Abraham M. de Vos,‡ and Robert F. Kelley*,‡

Departments of Protein Engineering, Research Bioassay, Bioanalytical Assay Technology, and Molecular Oncology, Genentech, Inc., 1 DNA Way, South San Francisco, California 94080

Received September 27, 1999; Revised Manuscript Received November 30, 1999

ABSTRACT: Apoptosis-inducing ligand 2 (Apo2L, also called TRAIL), a member of the tumor necrosis factor (TNF) family, induces apoptosis in a variety of human tumor cell lines but not in normal cells [Wiley, S. R., Schooley, K., Smolak, P. J., Din, W. S., Huang, C.-P., Nicholl, J. K., Sutherland, G. R., Smith, T. D., Rauch, C., Smith, C. A., and Goodwin, R. G. (1995) *Immunity 3,* 673−682; Pitti, R. M., Marsters, S. A., Ruppert, S., Donahue, C. J., Moore, A., and Ashkenazi, A. (1996) *J. Biol. Chem. 271,* 12687−12690]. Here we describe the structure of Apo2L at 1.3 Å resolution and use alanine-scanning mutagenesis to map the receptor contact regions. The structure reveals a homotrimeric protein that resembles TNF with receptor-binding epitopes at the interface between monomers. A zinc ion is buried at the trimer interface, coordinated by the single cysteine residue of each monomer. The zinc ion is required for maintaining the native structure and stability and, hence, the biological activity of Apo2L. This is the first example of metal-dependent oligomerization and function of a cytokine.

Apoptosis is essential for proper metazoan development and homeostasis (*1*). Apoptosis can be initiated by a variety of trimeric TNF[1] superfamily members including TNF (or TNF-α), LT (or LTα or TNF-*β*), and FasL, each of which appears to have a different specific function (*2*). These trimeric molecules initiate apoptosis by binding to related receptors, some of which possess intracellular death domains. The cell killing properties of these cytokines have made them exciting targets for drug development. Unfortunately, the inflammation they trigger is too indiscriminate to make them effective therapeutics. Apo2L (or TRAIL) is a recently characterized member of the superfamily (*3, 4*). Like most TNF family members, Apo2L is a type-II transmembrane protein that can be cleaved at the cell surface to form a soluble protein (*5*). Apo2L appears to be unique among TNF-related cytokines in that it selectively induces apoptosis in tumor cells while leaving normal tissue unscathed. Administration of soluble Apo2L to mice bearing human tumors reduces tumor size with no discernible toxicity to normal tissues (*6, 7*). The resistance of normal cells to the apoptosis-inducing effects of Apo2L may be explained in part by its regulation by a family of signaling and decoy receptors (*8*). Two signaling or "death" receptors (DR4, DR5) (*9*−*11*) and three nonsignaling or "decoy" receptors (DcR1, DcR2, OPG) (*9*−*12*) for Apo2L have been identified. These decoy receptors either lack functional intracellular death domains or are shed from the cell surface. Thus, Apo2L has potential as an anti-cancer agent in humans.

Prior structural information about the TNF superfamily is derived from the X-ray structures of TNF (*13, 14*), LT (*15*), and CD40L (*16*), which reveal that these cytokines are homotrimeric jelly roll proteins. TNF family members bind the extracellular portions of cysteine-rich receptors. Ligand-induced clustering of these receptors triggers the intracellular apoptotic cascade. From the structure of LT bound to TNFR1 (*17*), it was determined that the receptors bind to ligand monomer−monomer interfaces. Recently, a low resolution structure of Apo2L confirmed its general similarity to other TNF superfamily members (*18*). In addition, we and others have determined the structure of Apo2L bound to the ecto-domain of DR5 which shows an interface centered around Apo2L residues Gln 205 and Tyr 216 (*19, 20*).

Here we present the 1.3 Å crystal structure of the Apo2L/TRAIL trimer as well as the results of an extensive mutagenesis study elucidating the receptor-binding site. The structure reveals a novel zinc-binding site, which we show is required for proper Apo2L structure and function through a comprehensive series of biochemical and biophysical experiments. The mutagenesis analysis identifies at least five

* Corresponding author. Fax: 650-225-3734. E-mail: rk@gene.com.
‡ Department of Protein Engineering.
§ Department of Research Bioassay.
|| Department of Bioanalytical Assay Technology.
⊥ Department of Molecular Oncology.

[1] Abbreviations: Apo2L, apoptosis-inducing ligand 2; DR, death receptor; DcR, decoy receptor; LT, lymphotoxin; OPG, osteoprotegerin; rmsd, root-mean-square deviation; TNF, tumor necrosis factor; TNFR1, TNF p55 receptor; ICP-AES, inductively coupled plasma atomic emission spectrometry.

10.1021/bi992242l CCC: $19.00
Published on Web 01/04/2000

residues, distributed in two distinct patches, that are critical for high-affinity receptor binding and activity.

MATERIALS AND METHODS

Expression and Purification of Apo2L Mutants. Fragments of the extracellular domain of Apo2L corresponding to residues 91−281 or 114−281 were expressed in *Escherichia coli* and purified as previously described (*7*). Both fragments contain the entire region that is homologous to the receptor binding domain of TNF (Figure 2). The two fragments are equivalent for receptor binding, but the shorter form (114−281) is 1.5-fold more bioactive. Alanine substitution mutants of Apo2L were constructed by oligonucleotide-directed mutagenesis (*21*) of a plasmid (pAPOK5) designed for the intracellular *E. coli* expression of Apo2L (91−281) under control of the *trp* promoter. *E. coli* strain 294 transformed with the mutated plasmids were grown to mid-log phase at 37 °C in 250 mL of M9 media supplemented with 100 μM $ZnSO_4$ (no $ZnSO_4$ was added to the media for the production of protein used for crystallography), expression was induced by the addition of 25 μg/mL β-indole acrylic acid, and the cultures were grown overnight at 30 °C. Cells were harvested by centrifugation and frozen. The cell pellet was homogenized in 6 vol of 0.1 M Tris-HCl, pH 8, 0.2 M NaCl, 5 mM EDTA, and 5 mM DTT, and Apo2L was isolated from the soluble fraction by IMAC on a chelating hiTRAP column (Pharmacia) charged with nickel. Although the protein was not expressed with a histidine tag, Apo2L by itself has a weak affinity for immobilized metal and can be eluted with low concentrations of imidazole. A final purification was obtained by cation-exchange chromatography on an SP hiTRAP column (Pharmacia). Concentrations of purified Apo2L mutants were determined by absorbance measurements using an ϵ_{280} of 1.4 mg^{-1} mL cm^{-1}.

Crystallography. Crystals of wild-type Apo2L (114−281) were grown at 20 °C in 70 μL of sitting drops consisting of 40 μL of protein (at 2.6 mg/mL in 20 mM Tris, pH 8.0); 20 μL of 50 mM Tris, pH 8.0; and 10 μL of 8% poly(ethylene glycol) (PEG) 2K MME over a well solution of 50% PEG 2K MME. The space group was determined to be $P6_3$ with two monomers in the asymmetric unit and cell constants of $a = 72.5$ Å and $c = 140$ Å. These crystals are similar, but not identical, to Apo2L crystals reported recently (*22*). Crystals of Apo2L mutant Asp 218 Ala (residues 91−281 with Asp 218 mutated to alanine) grew at 4 °C in 14 μL of sitting drops containing 4 μL of 4% MPD and 10 μL of protein (1.7 mg/mL in 20 mM Tris-HCl, pH 7.5) over a well solution of 32% MPD. The space group was *R*32 with one monomer per asymmetric unit and cell parameters of $a = 66.4$ Å and $c = 197.7$ Å, and the crystals diffracted to a resolution of 1.3 Å at −180 °C with synchrotron radiation. Data sets to 3.9 Å resolution for the wild-type crystals and to 1.9 Å for the mutant were measured on a Rigaku rotating anode X-ray generator equipped with a MAR detector and processed with the program HKL (*23*). A 1.3 Å data set of the mutant was measured at the Structural Biology Center at Argonne National Labs and processed with HKL, giving $R_{merge} = 6.4\%$ (34% in the 1.35−1.30 Å shell), 100% completeness, 12-fold redundancy, and $\langle I/\sigma I \rangle = 12.4$. The wild-type structure was solved by molecular replacement using the program Amore (*24*) and a model based on TNF (PDB code 1TNF) and was refined (*25*) to an R_{free} of 33.5%. The mutant was initially refined against the 1.9 Å data set to an R_{free} of 25% and subsequently against the 1.3 Å data using Refmac (*23*) and SHELXL (*26*). During refinement, a 28σ peak of difference electron density was observed on the 3-fold axis near Cys 230 and modeled as a zinc ion; its B-factor refined to 11.8 Å^2. A fourth zinc ligand was identified on the trimer axis and refined as chloride ($B = 14.3$ Å^2). This ligand was tentatively identified as chloride after placing a water molecule at this position resulted in a refined B-factor of 4.0 Å^2 with a residual 7σ peak of difference electron density. The R and R_{free} are 14.1% and 19.7%, respectively, and the model has good stereochemistry with rms differences in bond lengths and angles of 0.014 Å and 2.54°. The final model consists of residues 120−130, 142−194, and 197−281 with 226 water molecules, one zinc ion, and one chloride ion. N-terminal sequencing and mass spectrometry analysis show that the protein used for crystallization was intact; therefore, the missing residues are presumably disordered. The coordinates for the Apo2L Asp 218 Ala structure have been deposited with the Protein Data Bank (access code 1DG6). Figures 1 and 4 were made with the programs Molscript (*27*) and Raster3D (*28*).

Determination of Receptor Binding Affinity. Dissociation constants (K_D) for the binding of Apo2L mutants to immobilized receptor immunoadhesions were determined from surface plasmon resonance measurements on a Pharmacia BIAcore 2000 (Pharmacia Biosensor, Piscataway, NJ). The receptor proteins were coupled to the sensor chip surface at a level of 500−1000 resonance units using the amine coupling chemistry (Pharmacia Biosensor). Sensorgrams were recorded for Apo2L binding at concentrations ranging from 15.6 to 500 nM in 2-fold increments. The kinetics constants were determined by nonlinear regression analysis according to a 1:1 binding model using software supplied by the manufacturer. Binding constants were calculated from the kinetic constants.

Bioactivity of Apo2L Mutants in Vitro. A bioassay that measures cell viability from the metabolic conversion of a fluorescent dye was used to determine the apoptotic activity of Apo2L variants. Serial 2-fold dilutions of wild-type or mutant Apo2L were made in RPMI-1640 media (Gibco) containing 0.1% BSA, and 50 μL of each dilution was transferred to individual wells of 96-well Falcon tissue culture microplates. (The formula for RPMI-1640 media does not include a zinc salt. The zinc concentration in this media is less than the detection limit for ICP-AES.) A total of 50 μL of SK-MES-1 human lung carcinoma cells (ATCC-CHTB58) (in RMPI-1640, 0.1% BSA) was added at a density of 2×10^4 cells/well. These mixtures were incubated at 37 °C for 24 h. At 20 h, 25 μL of alamarBlue (AccuMed, Inc., Westlake, OH) was added. Cell number was determined by measuring the relative fluorescence at 590 nm upon excitation at 530 nm. These data were analyzed by using a four-parameter fit to calculate ED_{50}, the concentration of Apo2L giving a 50% reduction in cell viability.

Metal Content of Apo2L. Elemental analysis of Apo2L was performed using inductively coupled plasma atomic emission spectrometry (ICP-AES) (*29*). The levels of Cd, Co, Zn, Ni, and Cu were determined in a 2 mg/mL solution of Apo2L (114−281) formulated in 20 mM Tris, pH 7.5, as well as in the formulation buffer. The standard error for these determinations was ±5%. For removal of the bound metal, a

sample of Apo2L was sequentially dialyzed versus 50 mM EDTA/2 mM 1,10-phenanthroline, and then versus metal-free 20 mM Tris, pH 7.5. After this treatment, a majority of the Apo2L migrated as a disulfide-linked dimer upon SDS−PAGE. For further analysis, the zinc-depleted Apo2L was reduced by incubation with 10 mM DTT for 1 h at ambient temperature followed by desalting on a PD-10 column (Pharmacia) equilibrated with PBS. Analysis by SDS−PAGE suggested complete reduction; however, the disulfide bonds were observed to slowly reform over a period of a few days at ambient temperature.

Circular Dichroic Spectroscopy. CD spectra were recorded on an Aviv model 202 circular dichroic spectrometer (Aviv, Inc.). Spectra were acquired at 25 °C on 20 μM solutions of protein, prepared in PBS, by using a step size of 0.5 nm and averaging time of 20 s. Quartz, rectangular cuvettes having a path length of 0.1 cm were used. Thermal denaturation experiments were performed using the same cuvettes and protein solutions. Measurements were made at 2 °C intervals following a 1-min equilibration period at the specified temperature. CD was measured at 222 nm using a 20-s averaging time. Simultaneously, fluorescence was recorded using a photomultiplier placed at a right angle to the CD path. The 222-nm light was used as the excitation source, and a 320-nm cutoff filter was placed in front of the photomultiplier tube to minimize stray light detection. The protein solutions were turbid upon cooling to ambient temperature, suggesting irreversible denaturation, and thus a rigorous thermodynamic analysis of the data was not performed.

Fluorescence Spectroscopy. Tryptophan fluorescence emission spectra were recorded on a SLM8000 spectrofluorimeter (SLM Instruments, Inc.). Spectra were obtained by using 1 μM protein solutions in PBS and rectangular quartz cells having a path length of 1 cm. Excitation was at 295 nm, and the emission spectrum was scanned from 305 to 400 nm using a 0.5-nm step size and a 1.0-s integration time.

RESULTS AND DISCUSSION

The X-ray structure of Apo2L was determined by molecular replacement using a model of TNF (*14*) and refined to 3.9 (wild type) and 1.3 Å (Asp 218 Ala mutant). Like other members of the TNF family, and as also confirmed by the low-resolution structure (*18*), Apo2L is a compact trimer formed of three jelly roll monomers that bury approximately 5100 Å^2 (1700 Å^2 per monomer) of solvent-accessible surface to form the globular trimer (Figure 1A). The structure is well defined, with the exception of a disordered N-terminal extension and two partially disordered loops. As expected from a low-resolution structure of Apo2L (*18*), the position of the core β-strands is well conserved as compared to the other structurally characterized members of the TNF family, TNF (*13*, *14*), LT (*15*), and CD40L (*16*), with a rms difference of 0.8 Å when superimposed on the strands of TNF or LT. Even though all TNF family members are expected to form trimers, none of the residues in the trimer interface are absolutely conserved; nevertheless, the hydrophobic character of the interface residues is preserved. The known structures are most similar at the top (the widest part of the trimer) and along the upper half of the 3-fold axis. Near the tip of the trimer interface, in the vicinity of Cys 230, the structures diverge considerably, especially in the conformation of the 190s and 230s loops.

In contrast to the invariant β-scaffold core, the structure of the loops and receptor binding surfaces varies significantly among the TNF family members. One major difference between the structures of Apo2L on one hand and TNF, LT, and CD40L on the other is the connection between strands A and A′. In TNF, LT, and CD40L, strand A is followed by a compact loop (see Figure 2). In Apo2L, a 15-residue insertion drastically lengthens this loop and alters its conformation. The first part of the loop (residues 131−141) is disordered while the second part (residues 142−154) crosses the surface of the molecule from one monomer−monomer interface to the next (Figure 1A) and has a conformation that resembles CD40L in its C-terminal portion.

A Novel Zinc-Binding Site Is Required for Structure and Function. An unanticipated finding in this structure is the presence of a novel zinc-binding site, buried near the tip of the trimerization interface. The three symmetry-related Cys 230 residues point inward toward the trimer axis and coordinate a metal ion in conjunction with an interior solvent molecule (possibly a chloride ion). This metal binding site exhibits a slightly distorted tetrahedral geometry with bonds and angles appropriate for a zinc-binding site and is completely inaccessible to solvent (Figure 1B). The identity of the bound metal was confirmed using inductively coupled plasma atomic emission spectrometry (ICP-AES (*29*)). In a quantitative analysis for Cd, Co, Zn, Ni, and Cu, 0.79 mol of Zn and 0.06 mol of Co per mol of Apo2L trimer were detected, showing that the bound ion in this structure is zinc with a stoichiometry of approximately one metal ion per trimer. Since zinc was not present in either the purification or crystallization buffer, the source must have been the *E. coli* intracellular pool or the growth media.

The functional importance of the zinc-binding site is demonstrated by the observation that alanine or serine substitution of Cys 230 results in 20- and 70-fold reductions in apoptotic activity, respectively (Table 1). Furthermore, removal of the bound metal from wild-type Apo2L by dialysis against chelating agents results in a significant decrease in receptor-binding affinity (Table 1) and a 90-fold decrease in apoptotic activity (Figure 3). Interestingly, upon removal of the zinc, the cysteines become prone to oxidation, and Apo2L forms poorly active, disulfide-linked dimers. Although native Apo2L can also form disulfide-linked dimers upon extended storage in the absence of reducing agents, the rate of oxidation is much faster for zinc-depleted Apo2L. Therefore, metal binding appears to play an indirect role in receptor binding and apoptotic activity since the zinc-binding site is buried and is not expected to contact the receptor. The variability in effect on apoptosis resulting from zinc depletion or Cys230 replacement (20−90-fold) probably reflects the energetic cost of burying a nonpolar residue (Ala) versus a polar residue (Ser or unliganded Cys).

Spectroscopic and melting temperature characterization of Apo2L show that zinc binding is important for maintaining the structure and stability of the Apo2L trimer. Far-ultraviolet CD spectra (Figure 4A) suggest a diminished β-sheet content for zinc-depleted Apo2L. Similarly, zinc-depleted Apo2L displays a 2.2-fold decreased tryptophan fluorescence relative to native Apo2L (Figure 4B). The decrease in fluorescence is consistent with a conformational change of Apo2L upon

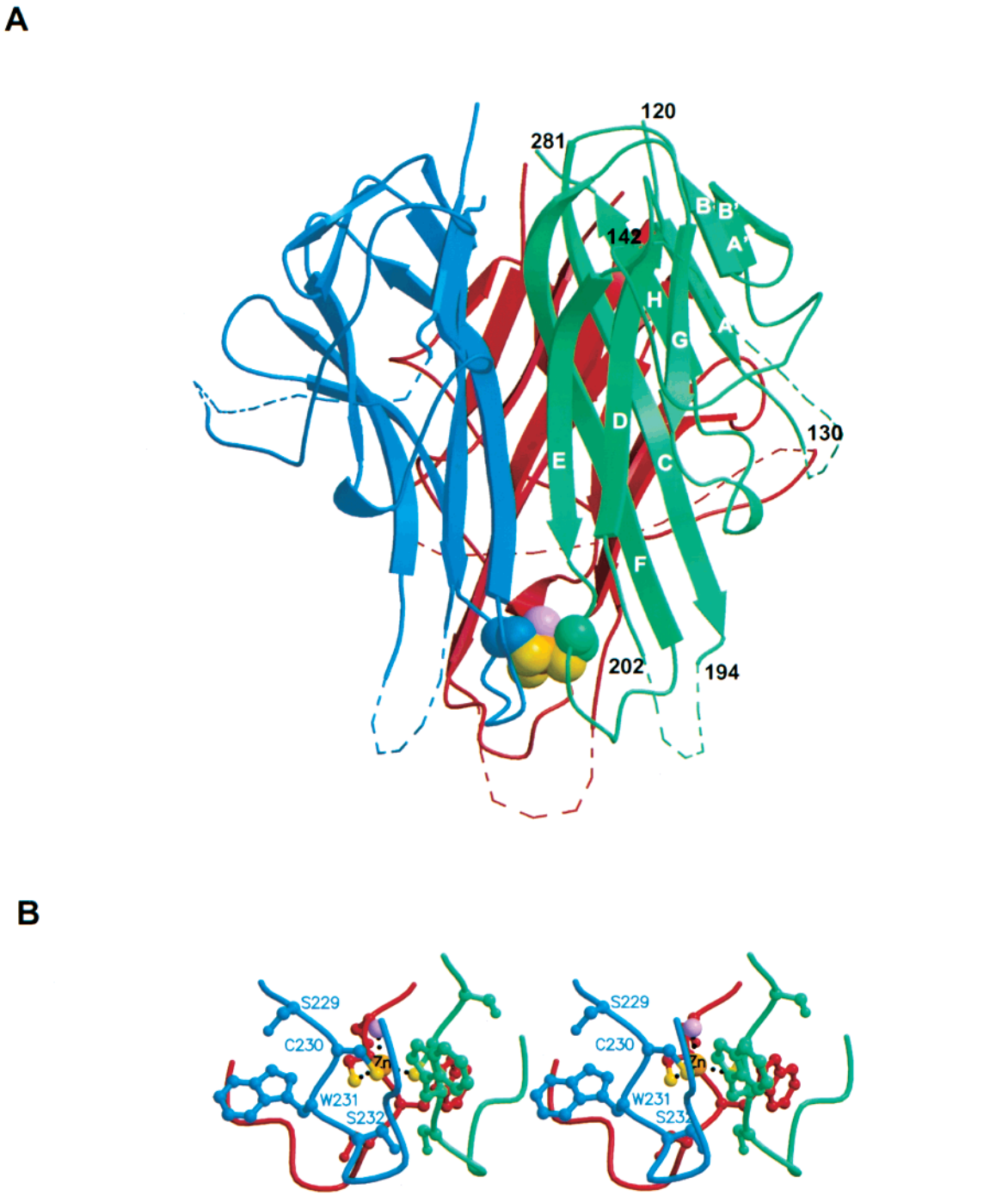

FIGURE 1: Overall structure of Apo2L. (A) View of the trimer perpendicular to the 3-fold axis. The ordered protein commences at residue 120. The two disordered, or marginally ordered, loops, residues 131−141 and 194−202, are marked with dashed lines. The zinc-binding site including the three symmetry-related cysteines and a putative chloride ligand are shown in space filling rendering. The sulfur atoms are yellow, the zinc is orange, and the chloride is pink. (B) Wall-eyed stereoview of the zinc-binding site; the angles between Sγ-zinc-Sγ are 114° and the Sγ-zinc-chloride angles are 107°, with 2.3 Å zinc-to-ligand bond distances.

loss of zinc resulting in increased solvent exposure of Trp 231, which is adjacent to the zinc-binding site (Figure 1B). The only other tryptophan residue in Apo2L, Trp 154, which is conserved among TNF family members (Figure 2), is buried in the core of the monomer far from the zinc-binding site and should be insensitive to the occupancy of the zinc-binding site. Addition of $ZnSO_4$ to the solution of zinc-depleted Apo2L results in a partial restoration of the tryptophan fluorescence (Figure 4B), suggesting that the conformational changes resulting from zinc removal are reversible. Conditions of zinc concentration, time, and temperature leading to a full recovery of fluorescence have not been determined. Thermal denaturation experiments show that zinc binding is important for the stability of Apo2L (Figure 4C). Both proteins display a cooperative unfolding transition, as detected by circular dichroism at 222 nm, but the melting temperature for zinc-depleted Apo2L is about 25 °C lower than measured for native Apo2L. Thermal denaturation of both proteins was irreversible, as a consequence of disulfide bond formation and aggregation, and thus ΔG values for unfolding were not determined. A cooperative thermal transition, coincident with the changes in circular

FIGURE 2: Sequence alignment of selected TNF family members. Residues that when mutated to alanine have a greater than 5-fold decrease on bioactivity are shown in red, residues that resulted in increased bioactivity are in purple, and cysteines are in green. Arrows over the sequence indicate β-strands in Apo2L. Conserved sections of the sequence are highlighted in blue. Numbering over the sequences refers to Apo2L sequence.

dichroism, is also observed by fluorescence measurements for native but not zinc-depleted Apo2L. These data indicate that removal of the zinc may cause an initial local unfolding of Apo2L that immediately exposes Trp 231 to solvent and also destabilizes the protein resulting in the shift in the melting temperature.

Since the zinc-binding site is located on the trimer axis, it is anticipated that the presence of zinc influences the trimerization constant. At the concentration limits of detection for dynamic light scattering and gel filtration monitored by absorbance at 280 nm, about 10 μM, both native and zinc-depleted Apo2L gave equivalent molecular weights consistent with a trimer (data not shown). Given the extensive monomer−monomer contact observed in Apo2L that is similar to other TNF family members, it is expected that zinc-depleted Apo2L is a relatively tight trimer. Indeed, gel filtration experiments with radiolabeled TNF, which does not have a zinc-binding site, show that the TNF trimer does not dissociate at concentrations as low as 10 nM (*30*). TNF also retains cytotoxic activity at concentrations less than 1 nM. Nonetheless, an increase in the trimer dissociation constant probably contributes to the lower thermal stability and decreased bioactivity measured for zinc-depleted Apo2L.

The Apo2L structure represents the first example of metal binding-mediated trimerization of a cytokine. This zinc-binding site is essential for full bioactivity. While zinc-binding sites have been shown to play structural roles in protein−protein interactions in many proteins involving diverse interfaces (*31*−*35*), none of the other structurally characterized members of the TNF family (CD40L, TNF, or LT) have metal-binding sites. On the basis of sequence analysis, the TNF family can be divided into three groups with respect to Cys 230 (see Figure 2). Some family members, such as LT and osteoprotegerin ligand, do not have a cysteine residue corresponding to Cys 230 of Apo2L. A second group, represented by TNF and Fas ligand, is characterized by the presence of a second cysteine residue in the loop adjacent to Cys 230 (the 194−203 loop in Apo2L), resulting in the formation of a disulfide bridge and precluding the formation of a metal-binding site. Finally, the only family members with an unpaired Cys 230 residue are Apo2L and its only known ortholog, murine Apo2L. In this regard, it is noteworthy that the conformation of the main chain immediately prior to Cys 230 in Apo2L differs from the disulfide-containing family members such as TNF and CD40L: in Apo2L, the side chain of Cys 230 is oriented toward the interface instead of away from it. Thus, the zinc-binding site confers unique structural and stability features to Apo2L differentiating it from all other TNF family members.

Table 1: Receptor Binding and Apoptotic Activity of Apo2L Mutants[a]

	ratio (mutant/wild-type)			
mutant	DR4-IgG K_D	DR5-IgG K_D	DcR2-IgG K_D	apoptosis ED_{50}
Δzinc	6.3	6.6	11.2	90.0
R130A	3	2.7	1.3	1.9
N134A	1.0	0.8	1.0	1.5
L136A	3.3	1.5	1.4	0.8
S138A	2.1	1.3	2.2	1.2
N140A	1.4	1.9	0.9	1.1
S141A	2.3	1.3	2.4	1.3
K142A	2.6	1.9	2.7	2.0
N143A	2.1	2.0	1.3	1.5
R149A	1.8	2.2	1.6	3.5
S153A	2.3	1.2	2.1	0.9
E155A	1.6	2	1.4	2.5
R158A	2.4	1.3	6.5	1.4
S159A	4.7	2.2	3.4	0.9
R170A	1.1	2.2	0.6	0.9
K179A	0.9	0.9	1.1	2.0
R191A	7.8	3.9	3.2	2.2
Q193A	1.7	1.1	1.2	2.2
E195A	4.6	1.4	2.6	0.8
K197D	2	2.1	2.9	1.1
K201A	4.3	2.7	10	2.5
N202A	2.5	2.5	1.9	3.2
D203A	1.5	1.1	0.6	0.5
Q205A	13.1	6.3	10.8	690
V207A	2.2	2.8	2.1	5.6
Y213A	1.3	1	1.5	1.2
Y216A	14.5	8.9	9.0	320
D218A	1.3	1.9	1.1	0.3
C230A	4.1	7.1	6.7	20
C230S	5.3	3.4	9.0	70
E236A	6.0	9.8	8.4	10.8
Y237A	7.3	5.0	48	8.3
Y240A	1.8	0.8	1.8	1.1
K251A	1.9	2	2.4	0.8
S259A	4.3	2.0	1.4	3.3
H264A	1.9	2.0	1.4	3.1
D267A	5.7	1.9	5.5	1.1
D269A	1.7	0.5	0.9	0.2

[a] Values shown represent the ratio of mutant to wild type. For wild-type Apo2L (91−281), the K_D values for DR4-IgG, DR5-IgG, and DcR2-IgG are 0.8 ± 0.3, 0.9 ± 0.4, and 0.3 ± 0.2 nM. The K_D measured for DR5 is consistent with results reported by Emery et al. (*12*). Wild-type Apo2L (91−281) gave an ED_{50} of 24.0 ± 3.1 ng/mL in the apoptosis assay while the 114−281 form of wild-type Apo2L was slightly more active and gave an ED_{50} of 16.0 ± 3.6 ng/mL. Only 2-fold and greater changes from wild-type values are considered to be significant.

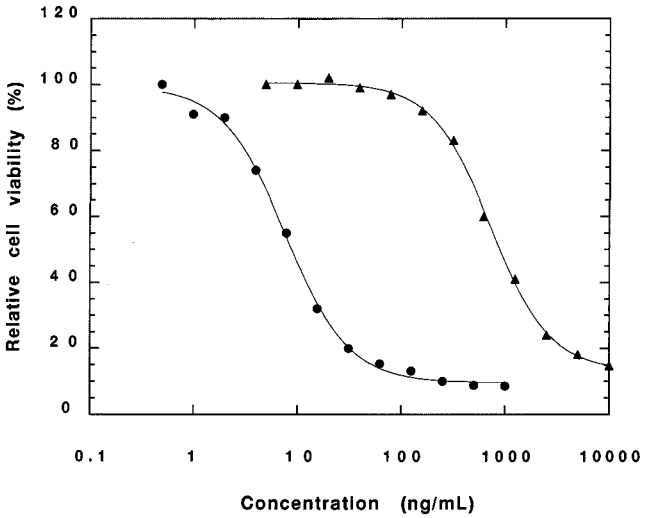

FIGURE 3: Bioassay data showing the functional importance of the zinc-binding site. Cell (SK-MES-1) viability was determined by a fluorescence assay of metabolic activity after overnight incubation with varying concentrations of wild-type Apo2L (114−281) (●) and wild-type Apo2L (114−281) treated with chelating agents to remove the zinc (▲).

Structural Effects of the Removal of Zinc. A comparison of our present structure to the three other known structures of Apo2L/TRAIL, namely, the low-resolution structure without zinc (*18*), the structure without zinc and bound to DR5 (*20*), and that of the complex with DR5 and containing zinc (*19*), reveals the effects of removing the zinc ion on the local structure of Apo2L. In the absence of zinc (*18*), the six residues following Cys 230 (including Trp 231) are disordered, and Cys 230 is described as being only 2.6 Å from its symmetry-related copies. In the zinc-depleted structure of the DR5-Apo2L complex, a disulfide bond is proposed to exist between two of the three symmetry-related cysteines (*20*). In addition, the 230s loop is very poorly ordered, as evidenced by the high-temperature factors in this segment (for example, the average B-factor for Cys 230 and Trp 231 is 100 and 142 Å^2, respectively, compared to an average of 50 Å^2 for the entire structure). The disorder in this loop in the zinc-depleted structures is consistent with our tryptophan fluorescence data, indicating that in the absence of zinc the Trp 231 side chain is likely solvent exposed (Figure 4B). In contrast, in the present, zinc-bound structure, the 230s loop is highly ordered with an average B-factor of only 36 Å^2, or about 10 Å^2 below the overall average. Furthermore, the conformation of this loop differs grossly from that observed in the absence of zinc, resulting in a buried and closely packed environment of Trp 231 in the zinc-bound trimer. It is noteworthy that the changes in loop conformation are propagated to Glu 236, resulting in changes in the receptor interactions for this side chain. In summary, the removal of zinc from Apo2L results in large conformational changes in the region near Cys 230, including potential mixed disulfide-bonded trimers and a partially exposed position of the side chain of Trp 231, which extend to the periphery of the receptor-binding site. The result of these changes may therefore include direct effects on receptor binding in addition to the marked destabilization of the structure revealed by our melting experiments.

The Receptor-Binding Site Shows Two Functionally Important Clusters of Residues. To map the receptor-binding site, amino acid residues important for binding and biological activity were identified by alanine-scanning mutagenesis (*36*). Residues were chosen for substitution on the basis of solvent accessibility and by analogy to the receptor contacts observed in the structure of the complex between LT and TNFR1 (*17*). Single alanine substitutions at five positions, residues Gln 205, Val 207, Tyr 216, Glu 236, or Tyr 237, resulted in a greater than 5-fold decreases in apoptotic activity in a bioassay (Table 1, Figure 5). Four of these five critical alanine substitutions (Gln 205, Tyr 216, Glu 236, and Tyr 237) resulted in at least a 5-fold decreased affinity for DR4, DR5, and DcR2. Of these residues, Gln 205 and Tyr 216 are the most critical in induction of apoptosis since alanine substitution at these two sites results in a greater than 300-

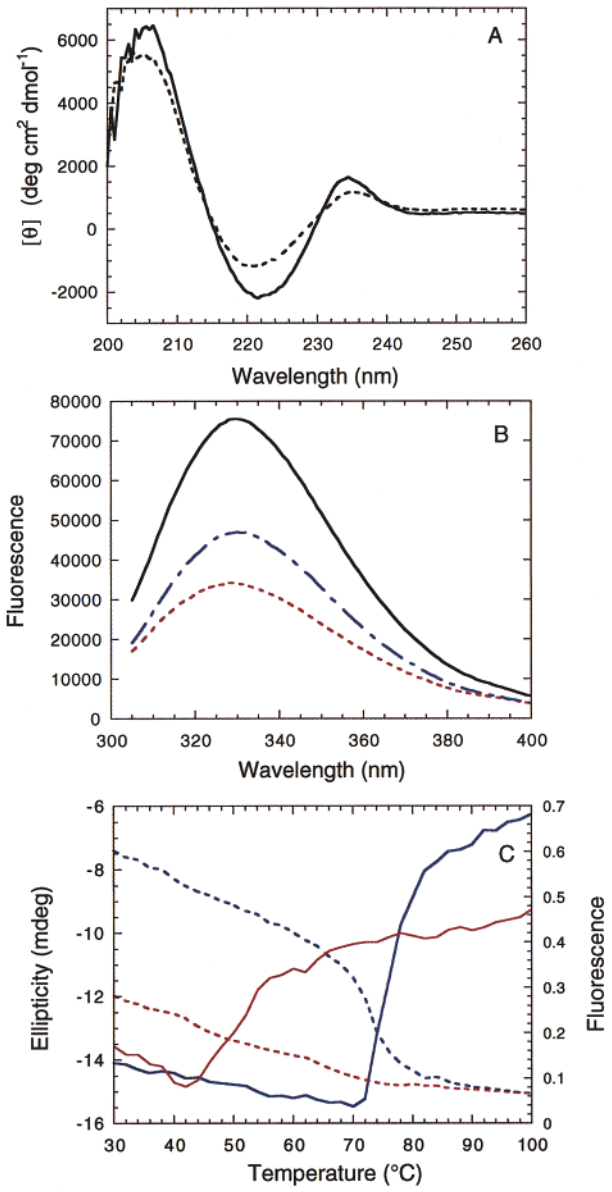

FIGURE 4: Effect of zinc removal on the conformation and stability of Apo2L. (A) Far-ultraviolet circular dichroic spectra of native (solid line) and zinc-depleted (dashed line) Apo2L. (B) Tryptophan fluorescence emission spectra of native (solid black line) and zinc-depleted (dashed red line) Apo2L. The spectrum observed after a 4-h ambient temperature incubation of zinc-depleted Apo2L with 50 μM $ZnSO_4$ is shown as the dot−dashed blue line. (C) Thermal denaturation of native (blue) and zinc-depleted (red) Apo2L. CD at 222 nm is shown as the solid lines, and fluorescence emission above 320 nm is shown as the dashed lines.

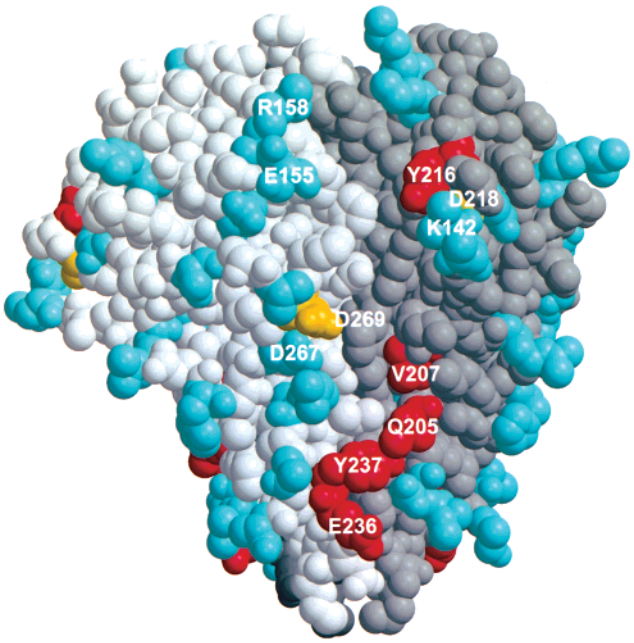

FIGURE 5: Mutational analysis of Apo2L. The trimer is oriented approximately as in Figure 1. Residues with a greater than 5-fold decrease or 2-fold increase in bioactivity when mutated to alanine are shown in red and yellow, respectively. Other residues mutated in this study are shown in cyan.

fold reduction in bioactivity. The mutant proteins with significantly reduced apoptotic activity also have impaired binding to both DR4 and DR5, suggesting that binding to at least one of these receptors is required for the biological effect.

In addition to the residues critical for apoptosis, many other alanine substitutions lead to small decreases (2−5-fold) in receptor-binding and apoptotic activity. Furthermore, alanine substitutions of Asp 218 or 269 resulted in 3−5-fold increases in apoptotic activity although neither mutation significantly affected receptor binding. Most of the minor deleterious alanine substitutions have similarly impaired binding to both DR4 and DR5, the only exceptions being mutation of Glu195 and Asp267, which have a pronounced effect on DR4 binding but a negligible effect on DR5 binding. Neither the E195A or D267A mutants of Apo2L have decreased apoptotic activity, suggesting that DR5 binding alone may be sufficient to induce apoptotic death in SK-MES-1 lung carcinoma cells upon Apo2L administration. Changes in DcR2 binding tend to parallel the effects observed for DR4 binding with the exception that alanine substitutions of Arg158 and Tyr237 have larger effects on DcR2 binding. Overall, these data suggest a similar contact region on Apo2L for DR4, DR5, and DcR2.

When the results of the mutagenesis analysis are mapped onto the structure, the functional epitope of Apo2L for receptor binding and biological activity is located along the walls of a surface crevice formed by adjoining monomers that runs from the wider part of trimer to the variable loops at the tip (Figure 5). This epitope is divided into two groups of residues: a concentrated patch of residues at the tip of the crevice and several other residues spread along the surface of the crevice at the wider part of the trimer. Each group provides an essential residue for signaling cell death, Tyr 216 at the top and Gln 205 at the tip of the trimer. Contact with these two residues appears to be crucial for organization of the receptors in the signaling complex since alanine substitution at these sites has a greater effect on apoptosis-inducing activity than on receptor binding. Apo2L residues Glu 155, Arg 158, and Tyr 216, at the top of the trimer, structurally correspond to TNF residues Leu 29, Arg 32, and Tyr 87, which have been shown to be critical for TNF receptor interactions (*37*−*39*). Similarly, residues in LT (*39*) and CD40L (*16*) important for receptor binding are also located on the wider part of the trimer. Many of these residues (Glu155 and Arg 158 in Apo2L, Asp 50 in LT, Arg 132 in TNF, and Lys 143 and Tyr 145 in CD40L) map to the C-terminal portion of the AA′ loop between strands A and A′. In contrast, the residues in TNF, LT, or CD40L that correspond to Apo2L residues Gln 205, Val 207, Glu 236, and Tyr 237 are not functionally important in these cytokines. In Apo2L these residues are crucial for receptor binding and biological activity and are located near the tip of the trimer in the more variable part of the structure (Figure 5). The result of these differences is that, while for TNF, LT, and CD40L the upper half of the trimer makes the most important contribution to receptor binding, additional key binding residues of Apo2L are found near the tip of the trimer, in the vicinity of the zinc-binding site. Therefore, the structural analysis of the mutagenesis data suggests that Apo2L has a larger and more extended contact surface for interaction with its target receptors than CD40L, TNF, or LT. The contact surface predicted by alanine scanning mutagenesis is in very good agreement with the interface observed in a crystal structure of Apo2L bound to DR5 (*19*).

In contrast to the well-characterized interaction between human growth hormone and its receptor (*40*), Apo2L does not present a "hot spot" epitope in which a few residues make a dominant contribution to receptor binding. None of the Apo2L alanine substitutions cause a greater than 20-fold reduction in affinity for DR4 or DR5, and the binding energy for Apo2L−receptor interaction appears to be more evenly distributed within the extended contact surface. This could be a consequence of Apo2L having evolved to recognize multiple receptors. Concentration of binding energy in a few residues might be incompatible with broad specificity for several receptors. One implication of these findings is that it may be very difficult to produce small molecule Apo2L mimetics since the overall binding interaction is built from multiple, weak interactions. Conversely, it may be possible to exploit the quantitative differences in receptor affinity shown here (Table 1) to engineer receptor selective variants of Apo2L. For example, a variant with greatly decreased DcR2 binding but only slightly diminished DR5 binding might be produced by combining substitutions at 158, 201, and 237. Receptor selective variants of Apo2L should be useful for further studies of the biological mechanism of action of this cytokine and might have interesting therapeutic profiles differing from those of the wild-type protein.

ACKNOWLEDGMENT

We thank Jake Tropea, Adrianne Kishiyama, and Jim Bourell for N-terminal sequencing and mass spectrometry; Ila Patel for ICP-AES; Roger Pai for providing the wild-type Apo2L (114-281) protein; Bob Pitti and Scot Marsters for supplying purified receptor immunoadhesins; Mark Vasser, Parkash Jhurani, and Peter Ng for oligonucleotide

synthesis; Audrey Goddard and Alan Zhong for DNA sequencing; Patricia Elkins for producing the first wild-type crystals; and Hans Christinger, Felix Vajdos, Christian Wiesmann, Charles Eigenbrot, Rongguang Zhang, and Frank Rotella for their assistance with synchrotron data collection at the APS. Use of the Argonne National Laboratory Structural Biology Center beamline at the Advanced Photon Source was supported by the U.S. Department of Energy

REFERENCES

1. Jacobson, M. D., Weil, M., and Raff, M. C. (1997) *Cell 88*, 347−354.
2. Nagata, S. (1997) *Cell 88*, 355−356.
3. Wiley, S. R., Schooley, K., Smolak, P. J., Din, W. S., Huang, C.-P., Nicholl, J. K., Sutherland, G. R., Smith, T. D., Rauch, C., Smith, C. A., and Goodwin, R. G. (1995) *Immunity 3*, 673−682.
4. Pitti, R. M., Marsters, S. A., Ruppert, S., Donahue, C. J., Moore, A., and Ashkenazi, A. (1996) *J. Biol. Chem. 271*, 12687−12690.
5. Mariani, S. M., Matiba, B., Armandola, E. A., and Krammer, P. H. (1997) *J. Cell Biol. 137*, 221−229.
6. Walczak, H., Miller, R. E., Ariall, K., Gliniak, B., Griffith, T. S., Kubin, M., Chin, W., Jones, J., Woodward, A., Le, T., Smith, C., Smolak, P., Goodwin, R. G., Rauch, C. T., Schuh, J. C. L., and Lynch, D. H. (1999) *Nat. Med. 5*, 157−163.
7. Ashkenazi, A., Pai, R. C., Fong, S., Leung, S., Lawrence, D. A., Marsters, S. A., Blackie, C., Chang, L., McMurtrey, A. E., Hebert, A., DeForge, L., Khoumenis, I. L., Lewis, D., Harris, L., Bussiere, J., Koeppen, H., Shahrokh, Z., and Schwall, R. H. (1999) *J. Clin. Invest. 104*, 155−261.
8. Ashkenazi, A., and Dixit, V. M. (1998) *Science 281*, 1305−1308.
9. Pan, G., Ni, J., Wei, Y. F., Yu, G., Gentz, R., and Dixit, V. M. (1997) *Science 277*, 815−818.
10. Pan, G., O'Rourke, K., Chinnaiyan, A. M., Gentz, R., Ebner, R., Ni, J., and Dixit, V. M. (1997) *Science 276*, 111−113.
11. Sheridan, J. P., Marsters, S. A., Pitti, R. M., Gurney, A., Skubatch, M., Baldwin, D., Ramakrishnan, L., Gray, C. L., Baker, K., Wood, W. I., Goddard, A. D., Godowski, P., and Ashkenazi, A. (1997) *Science 277*, 818−821.
12. Emery, J. G., McDonnell, P., Burke, M. B., Deen, K. C., Lyn, S., Silverman, C., Dul, E., Appelbaum, E. R., Eichman, C., DiPrinzio, R., Dodds, R. A., James, I. E., Rosenberg, M., Lee, J. C., and Young, P. R. (1998) *J. Biol. Chem. 273*, 14363−14367.
13. Eck, M. J., and Sprang, S. R. (1989) *J. Biol. Chem. 264*, 17595−17605.
14. Jones, E. Y., Stuart, D. I., and Walker, N. P. C. (1989) *Nature 338*, 225−228.
15. Eck, M. J., Ultsch, M., Rinderknecht, E., de Vos, A. M., and Sprang, S. R. (1992) *J. Biol. Chem. 267*, 2119−2122.
16. Karpusas, M., Hsu, Y.-M., Wang, J., Thompson, J., Lederman, S., Chess, L., and Thomas, D. (1995) *Structure 3*, 1031−1039.
17. Banner, D. W., D'Arcy, A., Janes, W., Gentz, R., Schoenfeld, H. J., Broger, C., Loetscher, H., and Lesslauer, W. (1993) *Cell 73*, 431−445.
18. Cha, S.-S., Kim, M.-S., Choi, Y. H., Sung, B.-J., Shin, N. K., Shin, H.-C., Sung, Y. C., and Oh, B.-H. (1999) *Immunity 11*, 253−261.
19. Hymowitz, S. G., Christinger, H. W., Fuh, G., Ultsch, M., O'Connell, M., Kelley, R. F., Ashkenazi, A., and de Vos, A. M. (1999) *Mol. Cell 4*, 563−571.
20. Mongkolsapaya, J., Grimes, J. M., Chen, N., Xu, X.-N., Stuart, D. I., Jones, E. Y., and Screaton, G. R. (1999) *Nat. Struct. Biol. 6*, 1048−1053.
21. Kunkel, T. A. (1985) *Proc. Natl. Acad. Sci. U.S.A. 82*, 488−92.
22. Cha, S.-S., Shin, H.-C., Choi, K. Y., and Oh, B.-H. (1999) *Acta Crystallogr. D55*, 1101−1104.
23. Otwinowski, Z., and Minor, W. (1997) *Methods Enzymol. 276*, 307−326.
24. Collaborative Computational Project, Number 4. (1994) *Acta Crystallogr. D50*, 760−763.
25. Brünger, A. T. *X-PLOR: version 3.1* (1987) Yale Press, New Haven, CT.
26. Sheldrick, G. M., and Schneider, T. R. (1997) *Methods Enzymol. 277*, 319−343.
27. Kraulis, P. J. (1991) *J. Appl. Crystallogr. 24*, 946−950.
28. Merrit, E. A., and Murphy, M. E. P. (1994) *Acta Crystallogr. D50*, 869−873.
29. Wolnik, K. A. (1988) *Methods Enzymol. 158*, 190−205.
30. Wingfield, P., Pain, R. H., and Craig, S. (1987) *FEBS Lett. 211*, 179−184.
31. Feese, M., Pettigrew, D. W., Meadow, N. D., Roseman, S., and Remington, S. J. (1994) *Proc. Natl. Acad. Sci. U.S.A. 91*, 3544−3548.
32. Somers, W., Ultsch, M., de Vos, A. M., and Kossiakoff, A. A. (1994) *Nature 372*, 478−481.
33. Raman, C. S., Li, H., Martasek, P., Kral, V., Masters, B. S., and Poulos, T. L. (1998) *Cell 95*, 939−950.
34. Chothia, C., Lesk, A. M., Dodson, G. G., and Hodgkin, D. C. (1983) *Nature 302*, 500−505.
35. Weiss, M. A., Hua, Q.-X., Lynch, C. S., Frank, B. H., and Shoelson, S. E. (1991) *Biochemistry 30*, 7373−7389.
36. Cunningham, B. C., and Wells, J. A. (1989) *Science 244*, 1081−1085.
37. Van Ostade, X., Tavernier, J., and Fiers, W. (1994) *Protein Eng. 7*, 5−22.
38. Yamagishi, J., Kawashima, H., Matsuo, N., Ohue, M., Yamayoshi, M., Fukui, T., Kotani, H., Furuta, R., Nakano, K., and Yamada, M. (1990) *Protein Eng. 3*, 713−179.
39. Goh, C. R., Loh, C. S., and Porter, A. G. (1991) *Protein Eng. 4*, 785−791.
40. Clackson, T., and Wells, J. A. (1995) *Science 267*, 383−386.

BI992242L